Design proposal for Ridge Gap Waveguide and comparison with other technologies in Ka to W bands

A. Tamayo Domínguez , J.M. Fernández González , J.M. Inclán Alonso , M. Sierra-Pérez

***Abstract*—A design procedure of Ridge Gap Waveguide technology is proposed. The simulated results for Ka-band and above are compared with other technologies like Substrate Integrated Waveguide, microstrip or classical waveguide in terms of transmission losses.**

***Index Terms*—ridge gap waveguide design, high frequency technologies, Ka band, V band, W band, transmission losses, substrate integrated waveguide, ridge gap waveguide, 5G.**

I. INTRODUCTION

The arrival of 5G services demands the use of an increasing bandwidth, which leads to better use of the electromagnetic spectrum. However, the spectrum is widely occupied by other services up to K-band frequencies. Therefore, it is inevitable to use technologies that make the use of spectrum be feasible at Ka-band frequencies and above. 5G mass deployment requires solutions for working in desired frequency bands with low cost manufacturing. Printed substrate based technologies are good candidates. Nevertheless, printed substrate technologies, as stripline or microstrip, exhibit high transmission losses at high frequencies due to the presence of dielectric. At high frequencies, printed technologies have been replaced by waveguide. This technology is based on electromagnetic waves propagation in a rectangular, cylindrical or elliptical metal cavity, which suppose extremely low transmission losses. However, materials and manufacturing mechanisms are expensive and the resulting structures are heavy and bulky. This makes waveguides incompatible with the development and mass production of small and low cost technology.

In recent years various technologies have been emerged, such as Substrate Integrated Waveguide (SIW) or Ridge Gap Waveguide (RGW), that present the solution through printed structures that emulate the waveguides. These new technologies are becoming globally important because they offer good performance in terms of low weight, low profile and low losses, and a low cost fabrication on a massive scale over other printed technologies or classical waveguides. The SIW technology involves synthesizing a substrate integrated structure with a similar waveguide behavior. To this end, it is used metallized via holes which connect the upper and lower metal plates of the substrate, so that it is obtained a path in which the wave propagates [1][2]. As for the RGW technology, it tries to solve the dielectric losses problems that occur at high frequencies in SIW, due to the wave propagation within a dielectric substrate. RGW uses a waveguide with a central ridge on which the side walls are replaced by a metamaterial surface. This surface prevents the transmission of power in the transverse direction and confines the wave around the central ridge [3][4]. Both technologies have to undergo a process of maturation and consolidation to meet new 5G needs.

The main objective of this paper is to propose a design procedure for RGW technology in a given frequency band and to compare the transmission losses at high frequencies between different technologies.

II. RGW DESIGN

The design of Ridge Gap Waveguide is still more laborious than SIW, which derives from a well-known procedure [5]. RGB is based on the use of metamaterial that blocks the transmission of the fields along the transversal direction, concentrating it in the longitudinal direction guided by a metal ridge.

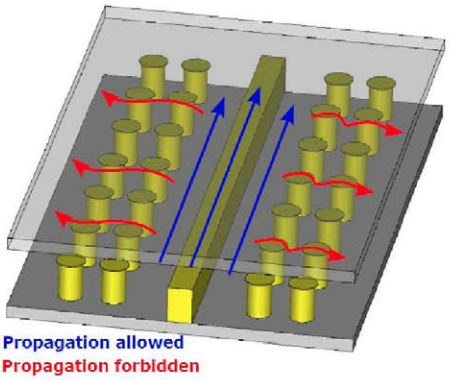

Fig. 1. RGW scheme design. Source: [6]

Methods for designing of ridge waveguide [7], SIW and PEC over PMC based on metamaterials [8] are combined.

A. PEC over PMC

First of all, it is chosen the desired frequency band that will be used. The transversal propagation in this band must be forbidden, which is achieved when the metamaterial structure, based on a bed of nails, behaves like PMC. As approximation, TM modes are forbidden when the height of the via holes d in

the dielectric is λ/4, where λ is the wavelength in the dielectric. TE modes cannot propagate if the total dimension between metal plates is $b=d+h<\lambda/2$, which corresponds to the cutoff frequency of the first TE mode. In this case, we have two different mediums and the cutoff frequency is an approximation valid if $h<<d$ due to $\varepsilon_{eff}\simeq\varepsilon_r$. If this condition is not fulfilled, it can be used a better approximation based on an inhomogeneously filled parallel-plate transmission line found in [9]. This creates an artificial PEC over PMC surface which blocks the propagation when the air gap h between them is typically smaller than λ/4. A detailed analysis of this bed of nails structures is found in [10], [11] and [12].

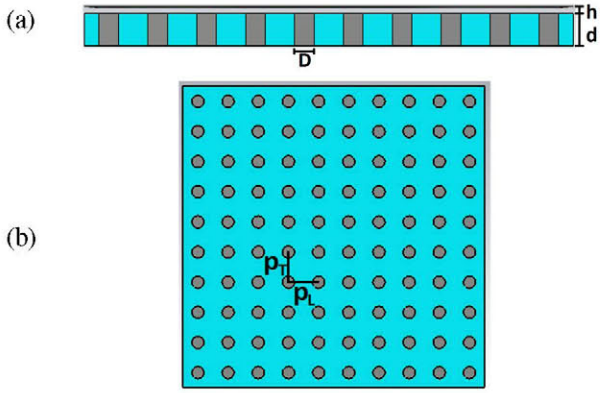

Fig. 2. Metamaterial structure. Front view (a) and top view (b).

In Fig. 2, h is the air gap between PEC and PMC metamaterial surfaces, d is the thickness of the dielectric substrate used to perform the PMC surface, D is the diameter of the via holes in the dielectric metamaterial, p_L is the periodic longitudinal separation of the vias and p_T is the periodic transversal separation between them. It is performed some simulations sweeping the d and h parameters with CST in order to determine the effect of the variations in each of them, using RO4350B substrate (ε_r = *3.66*). The dimensions for p_L, p_T, and D will be calculated on the basis of empirical results.

1) Dielectric thickness d sweep (h=1mm;p=0.5mm;D=0.2mm)

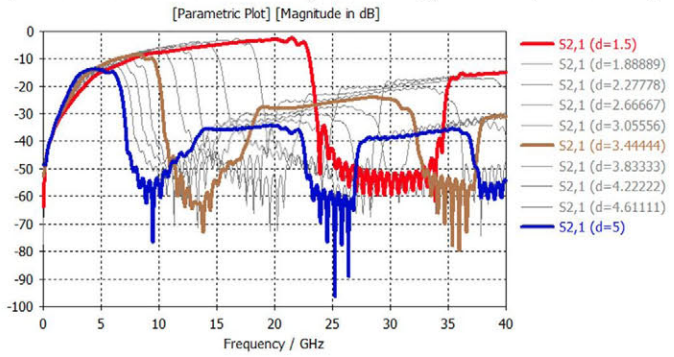

Fig. 3. Stop band on RGW depending on the dielectric thickness.

In Fig. 3, it is shown the stop bands in the dispersion grid, which are found in the corresponding frequencies around odd multiples of a quarter wavelength in the dielectric substrate d in *mm*.

In the next figures, it is represented the starting and ending frequencies of the first stop band, and the relation between the dielectric thickness and the wavelength in the effective medium.

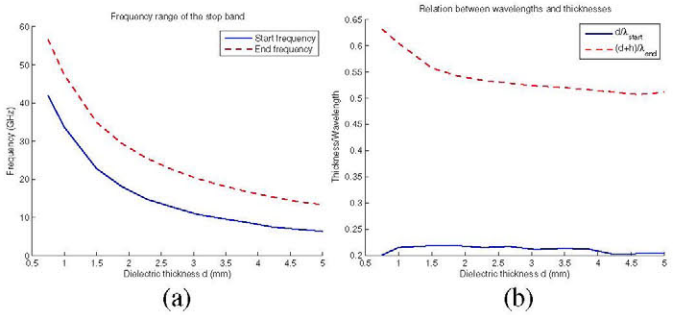

Fig. 4. Start and end cutoff frequencies (a) and the equivalent wavelength in the dielectric (b). Dielectric thickness sweeping.

It is tested that the band gap moves in frequency with a relation of approximately 0.25 between the dielectric thickness and the wavelength for the start frequency and 0.5 between the sum of the dielectric thickness and the air gap and the wavelength for the end frequency. The curves in Fig. 4 differ slightly from the theoretical values because the structure begins or ends stopping the fields also at near frequencies. The approximation applied in the calculation of λ_{end} is worse for small values of d because of the difference between ε_{eff} and ε_r is not negligible (Fig. 4 (b)).

2) Gap thickness h sweep (d=1.5 mm; p=0.5mm;D=0.2mm)

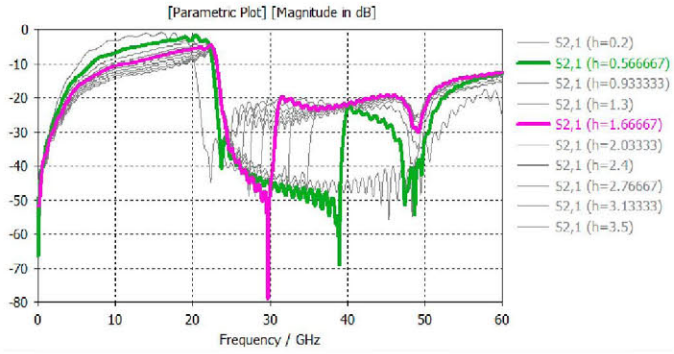

Fig. 5. Stop band on RGW depending on the air gap thickness.

The band is wider for smaller values of the air gap h, as Fig. 5 shows, due to the value of $b=d+h$ is smaller and then the cutoff frequency of the first TE mode increase. The frequency band is represented depending on h in Fig. 6.

The relations between medium thicknesses and the wavelength in the medium are maintained to 0.25 and 0.5 respectively. As the value of h increases, the wavelength and total thickness relation separates from the 0.5 value due to the fact that the effective dielectric constant changes and the approximation to ε_r is not valid (Fig. 6 (b)).

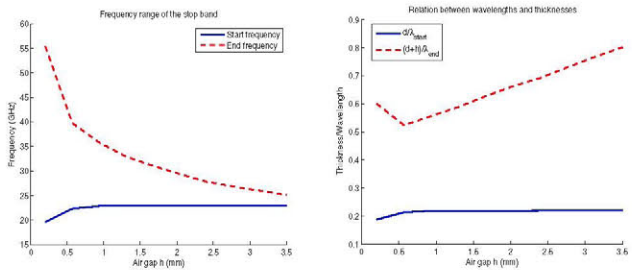

(a) (b)

Fig. 6. Start and end cutoff frequencies (a) and the equivalent wavelength in the dielectric (b). Air gap thickness sweeping.

The stop bandwidth limit occurs when h tends to 0, being the final stop frequency one octave above the initial frequency. In this case, the limits are 26.13 GHz and 52.3 GHz, although in Fig. 6 (a) they are a bit different because the structure stops fields also when frequency is approaching those limits.

Then, the selection of d and h is based on the equations (2) and (3).

$$d = \lambda_{start}/4 \quad (2)$$

$$b = d + h = \lambda_{end}/2 > \lambda_{start}/2 \quad (3)$$

Being:

$$\lambda_{start} = \frac{c}{f_{start}\sqrt{\epsilon_r}} \text{ and } \lambda_{end} = \frac{c}{f_{end}\sqrt{\epsilon_{eff}}} \simeq \frac{c}{f_{end}\sqrt{\epsilon_r}} \; if \; h \ll b$$

Nevertheless, the relation h/b will affect the design of the ridge waveguide in the next step. Apart from that, the value of d must be a standardized thickness given by the substrate manufacturer, which is RO4350B in this case. The election must have this in account, so it is chosen a stop band centered in 32 GHz with limits in 25.7 GHz and 40 GHz. The results for the variation of dielectric and gap air thicknesses are similar to those obtained in [12]. As explained in [12], the relation between the radius of the pins $r=D/2$ and their periodicity $p=p_T=p_L$ both in transversal and longitudinal directions determines the final bandwidth of the stop band. In Fig. 6 and Fig. 8 in [12], a maximum bandwidth has been obtained for values of r/p from 0.05 to 0.2 depending on the air gap h. Also, a maximum bandwidth occurs when the radius is about $0.075\lambda_0$, with λ_0 at the central frequency of the stop band (f_0 = 32 GHz) in the dielectric substrate. The obtained values are shown in Table I.

TABLE I. DESIGN PARAMETERS FOR PEC OVER PMC METAMATERIAL

Design parameters		
d=1.524 mm	*h=0.4 mm*	*h/b≈0.2*
r=0.075λ₀=0.36 mm	*r/p=0.15*	*p=2.5 mm*

B. Ridge waveguide

The design of the ridge waveguide depends on four parameters shown in Fig. 7.

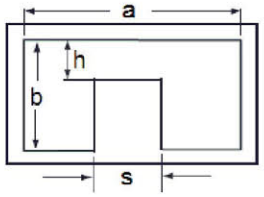

Fig. 7. Ridge waveguide paremeters.

The calculations are found in [7] and it summarizes the results in different curves depending on the cutoff wavelength of the TE_{10} mode in the ridge waveguide. It is necessary to consider that using a metalized substrate supposes a reduction of the air gap over the ridge, due to a copper foil which is added over the substrate. The thickness of this foil is 0.035 mm in this case, so the actual value of air gap is *h=0.365 mm.*

From Fig.5 in [7] it can be obtained the values of a and s for a standard relation b/a=0.45. If the relation b/a is different it must be applied a correction given by Fig. 8 in [7]. Fig.5 relates the values of h/b, s/a and λ_c/a. This leads to a four way trade-off. For values of h/b smaller than 0.2 the curves have a rapid variation, which implies that a small error in the manufacturing may produces important deviations in the final result. For values higher than 0.3 the slope of the curves is small, but the effective permittivity constant between dielectric and air cannot be approximated by the permittivity in the dielectric and the real λ_c will be different. For the s/a parameter it is convenient those values in which the slope of the curves are near to zero in order to avoid several manufacturing deviations. Also, the value of λ_c/a, which is maximum in zero slope neighborhood, is better the bigger due to the final design will have a reduced size for a given cutoff frequency. The b/a value affects to the final cutoff frequency due to bigger values than the standard 0.45 suppose an increment of the final corrected λ_c/a parameter, and smaller values suppose a decrement. Finally, after a trade-off analysis it is possible to obtain all the design parameters of the ridge waveguide. λ_c will be calculated with a dielectric constant equals to unity because the main part of the field energy is propagated above the ridge in the air gap. It is chosen a cutoff frequency of f_c=20 GHz in order to the propagation occurs at the frequencies of the dispersive PEC over PMC stop band. The bandwidth of the ridge waveguide is wider than the conventional rectangular waveguide, so there are no problems due to the propagation of higher modes until the 40 GHz limit of the band stop. It is obtained the results shown in Table II:

TABLE II. DESIGN PARAMETERS FOR RIDGE WAVEGUIDE

Choice of parameters			
h/b=0.2	*λ_c=c/f_c=15mm*	*b/a=0.55*	*λ_c/a=4.29*
$\lambda_c/a = \lambda_c/a_0 + (b/a-0.45)\cdot F_0$ where λ_c/a_0 and F_0 depend on s/a			
Values from curves in Fig.5, Fig.6, Fig.7 and Fig. 8 in [2]			
*Choice of s/a to obtain the desired λ_c/a: **s/a=0.5; F_0=0.9** (h/b=0.2)*			
λ_c/a_0=4.2 (TE_{10})	*λ_{c1}/a_0=1.3 (TE_{20})*	*λ_{c2}/a_0=0.9 (TE_{30})*	
Corrected values adding (b/a-0.45)·F_0=0.09 correction			
λ_c/a=4.29 (TE_{10})	*λ_{c1}/a=1.39 (TE_{20})*	*λ_{c2}/a=0.99 (TE_{30})*	
Final ridge waveguide parameters			
a=3.5 mm	*s=1.75 mm*	*b=1.924 mm*	*h=0.365 mm*

High order modes cutoff frequencies	
$f_c(TE_{20})$=61.7 GHz	$f_c(TE_{30})$=86.6 GHz

Cutoff frequencies for higher modes are above the desired band, so the fundamental mode propagation will not be affected.

C. *Bed of nails and ridge waveguide combination over dielectric substrate. A SIW approach.*

The next step is to determine the separation between the bed of nails design and the central ridge. The internal structure scheme is shown in Fig. 8.

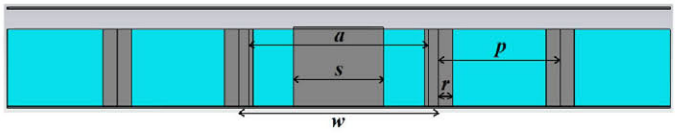

Fig. 8. Front view of ridge gap waveguide. Relation between ridge waveguide and bed of nails structure.

Having this in account, it is used the design expression for SIW (4).

$$a = w_{eff} = w - \frac{4r^2}{0.95 \cdot p} \tag{4}$$

Being w_{eff} the width of the waveguide and w the width of the equivalent SIW. w_{eff} is supposed to be equal to the ridge waveguide width a=3.5 mm. r and p parameters have already been obtained (r=0.37mm and p=2.5mm). The design separation value w between first rows of lateral nails is shown in Table III.

TABLE III. BED OF NAILS AND RIDGE RELATION

Design parameters			
w_{eff}=3.5 mm	r=0.37 mm	p=2.5 mm	w=3.73 mm

This is obvious that for a compact design it should be used a reduced number of pins rows for the bed of nails structure. As a first approximation it is used only two rows in each side of the ridge, considering that the variation of the metamaterial behavior will be negligible.

The ridge cannot be a solid piece of metal because of it is used a dielectric substrate. Then, the solid ridge is substituted by a row of metallized via holes that connect a strip over the dielectric with the bottom metal plate.

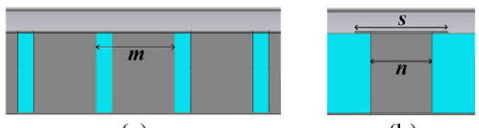

Fig. 9. Internal structure of the ridge for substrate-based manufacturing. Lateral view (a) and front view (b).

In Fig. 9 (a) and (b) it is shown the internal structure of the ridge. The m parameter corresponds to the periodic separation between pins and n is their diameter. In the manufacturing process some metal can exceed the border of the via hole, so the diameter should be smaller than de ridge width. Meanwhile, the separation gap between via holes should be smaller than the minimum wavelength in the working band in order to the ridge seems homogeneous. The values for m and n have been chosen in Table IV:

TABLE IV. DESIGN PARAMETERS FOR INTERNAL STRUCTURE OF RIDGE

Central ridge structure	
$n=s\cdot 3/4$=1.3 mm	$m=n\cdot 5/4$=1.64 mm
m-n=0.34 mm<<λ_{min}=3.9 mm	

With this step, the design of the ridge gap waveguide for the desired band of frequencies have concluded. Now, a simulation of the design is performed in CST.

III. RGW RESULTS

The RGW has been modeled in CST with the obtained parameters and a total length of L = 36 mm, which is about two times the largest wavelength in the band.

Fig. 10. Results of the RGW design.

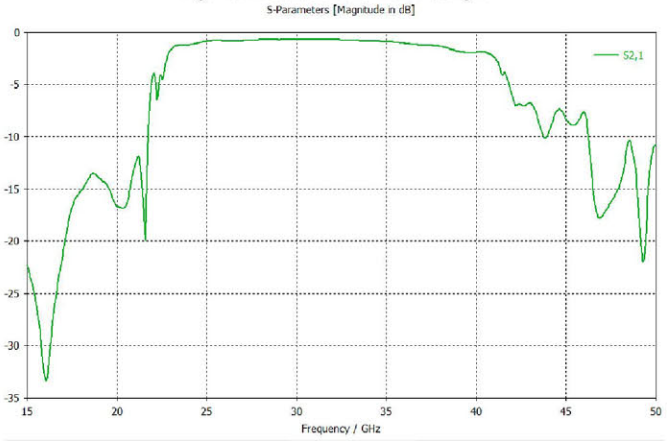

The expected band goes from 25.7 GHz and 40 GHz, but, as it is said, the radius and separation between pins have been selected in order to increase the bandwidth. Because of this, the simulated band is wider from 22.5 GHz and 41.4 GHz at 3 dB.

IV. COMPARISON BETWEEN TECHNOLOGIES

The main objective of this paper is to compare the transmission losses between RGW, SIW, rectangular waveguide and microstrip technologies at high frequencies. Different models of each technology have been designed and simulated in order to obtain their losses per unity of length in function of the frequency. It has been used a dielectric with dielectric constant ε_r=3.66 and loss tangent $tan\delta$=0.0037 (RO4350B substrate). It is considered that both parameters ε_r and $tan\delta$ are constant in frequency. Curves for air-filled and dielectric-filled have been plotted for SIW and waveguide. The results are shown in Fig. 11 (a) and (b).

Microstrip (MS), SIW over dielectric and dielectric-filled waveguide (WG) show similar results due to high losses in the dielectric when frequency increases. SIW over air and air-filled waveguide show the best results with losses lower than 0.02 dB/cm but manufacturing process is more expensive than solutions based on printed technologies over dielectric substrate.

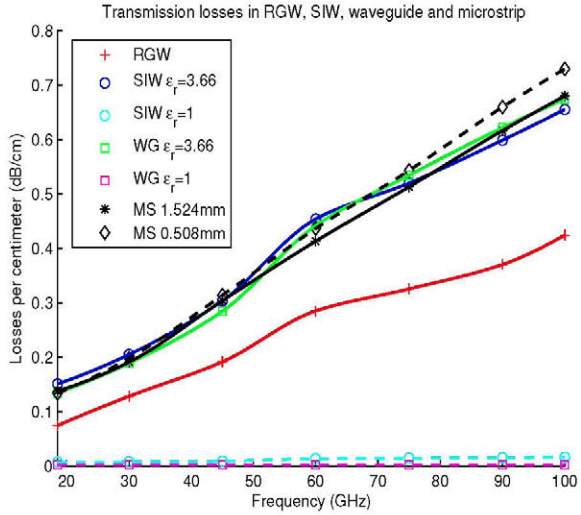

Fig. 11. (a) Comparison of transmission losses between RGW, SIW, rectangular waveguide and microstrip.

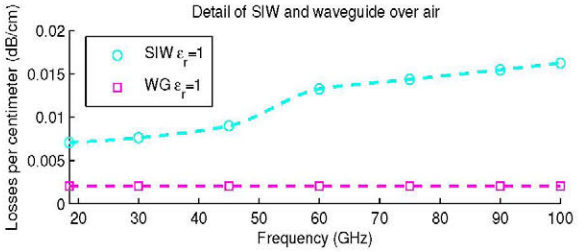

Fig. 11. (b) Detail of transmission losses in SIW over air and air-filled waveguide.

It is found that RGW technology provides better results than SIW when dielectric substrate is employed. This is because most of the energy in RGW is propagated through the air gap over the ridge and, in consecuence, dielectric losses are much smaller than in SIW. However, losses due to the central ridge conductor increase with frequency and it is not possible to achieve losses levels comparable to SIW over air.

Prototype construction and measured results will be presented in EuCAP 2016 Conference in Davos, Switzerland.

V. Conclusions

The research of inexpensive technologies that provide low transmission losses at frequencies in Ka band and above is one of the main objectives to address the challenges arising from the development of 5G. In this paper, different technologies have been compared at high frequencies. Among them, RGW stands out due to its low losses versus easy and low cost manufacturing relation. It is also proposed a design procedure of RGW in order to achieve those low losses properties in the desired frequency band.

Acknowledgment

Simulations done in this work have been performed using CST Microwave Studio Suite 2015 under a cooperation agreement between Computer Simulation Technology (CST) and Technical University of Madrid. The authors want to acknowledge the Spanish Government, Ministry of Economy, National Program of Research, Development and Innovation for the support of the project ENABLING5G "Enabling Innovative Radio Technologies for 5G networks" (Project number TEC2014-55735-C3-1-R) and the project Spacer Debris Radar from Madrid Region Government (Project number S2013/ICE-3000SPADERADAR-CM). Acknowledgement to FPI grant with reference BES-2015-075230.

References

[1] M. Bozzi, L. Perregrini, K. Wu and P. Arcioni, "Current and future research trends in substrate integrated waveguide technology," Radioengineering, 2009, vol. 18, no 2, p. 201-209.

[2] T. Djerafi and K. Wu, "Substrate integrated waveguide (SIW) techniques: The state-of-the-art developments and future trends," Journal of University of Electronic Science and Technology of China, 2013, vol. 42, no 2, p. 171-192.

[3] E. Alfonso, A. Valero, J.I. Herranz, M. Baquero, M. Ferrando, V. Rodrigo, F. Vico, E. Antonino, M. Cabedo, D. Sánchez, B. Bernardo, A. Vila, "New waveguide technology for antennas and circuits," Waves, year 3, ISSN 1889-8297, 2011,pp. 65-75.

[4] E. Alfonso, M. Baquero, P.-S. Kildal, A. Valero-Nogueira, E. RajoIglesias, and J. I. Herranz, "Design of microwave circuits in ridge-gap waveguide technology," in Proc. IEEE MTT-S Microw. Symp. Dig., May 2010, pp. 1544–1547.

[5] F. Xu and K. Wu, "Guided-wave and leakage characteristics of substrate integrated waveguide," Microwave Theory and Techniques, IEEE Transactions on, 2005, vol. 53, no 1, p. 66-73.

[6] J.M. Inclán, M. Sierra. "Planar reconfigurable antennas for satellite communications," ETSI. Telecomunicación. Universidad Politécnica de Madrid, Doctoral Thesis, 2015.

[7] S. Hopfer, "The design of ridged waveguides," IEEE Transactions on Microwave Theory and Techniques, 1955, vol. 3, no 5, p. 20-29.

[8] E. Alfonso, P.-S. Kildal, A. Valero-Nogueira and J. I. Herranz. "Numerical analysis of a metamaterial-based ridge gap waveguide with a bed of nails as parallel-plate mode killer," En Antennas and Propagation, 2009. EuCAP 2009. 3rd European Conference on. IEEE, 2009. p. 23-27.

[9] R. E. Collin. "Foundations for microwave engineering," John Wiley & Sons,p.117, 2007.

[10] A. Polemi, S. Maci and P.-S. Kildal. "Dispersion characteristics of a metamaterial-based parallel-plate ridge gap waveguide realized by bed of nails," Antennas and Propagation, IEEE Transactions on, 2011, vol. 59, no 3, p. 904-913.

[11] P.-S. Kildal, E. Alfonso, A. Valero-Nogueira, E. Rajo-Iglesias. "Local metamaterial-based waveguides in gaps between parallel metal plates," Antennas and Wireless Propagation Letters, IEEE, 2009, vol. 8, p. 84-87.

[12] E. Rajo-Iglesias. P.-S. Kildal. "Numerical studies of bandwidth of parallel-plate cut-off realised by a bed of nails, corrugations and mushroom-type electromagnetic bandgap for use in gap waveguides," IET microwaves, antennas & propagation, 2011, vol. 5, no 3, p. 282-289.